International Journal of Offshore and Coastal Engineering
Vol.10 | No. 1 | pp. 7 – 14 | May 2026
e-ISSN: 2580-0914

Submitted: December 12, 2025 | Revised: February 20, 2026 | Accepted: March 6, 2026

Mooring Chain Fatigue Analysis at the Single Point Mooring Ardjuna Marine Terminal Due to the Combination of Wave, Current, and Wind Loads Using the Fracture Mechanics Method

Rafi Manaf Mawardi[a*], Daniel Mohammad Rosyid [a], and Rudi Waluyo Prastianto[a], Raditya Danu Riyanto[a]
[a)] Department of Ocean Engineering, Institut Teknologi Sepuluh Nopember, Surabaya, Indonesia
*Corresponding author: rafimanafmawardi05@gmail.com

ABSTRACT

Mooring chain failure in Single Point Mooring (SPM) systems is a critical risk in offshore operations due to cyclic and complex environmental loading. The combination of waves, currents, and winds produces stress fluctuations that trigger crack initiation and propagation that can potentially lead to structural failure. This study analyzes the fatigue behavior of mooring chains in SPM at Ardjuna Marine Terminal, Java Sea, using a fracture mechanics approach. Cracks are modeled as semi-elliptical surface cracks, and the crack propagation rate is predicted using Paris Law based on Stress Intensity Factor (SIF) evaluation through numerical simulations. The motion responses of SPM and FSO are analyzed using Executive software, while the mooring chain stress analysis is performed using Dynamic simulation software. The results show a maximum SIF value of 1821.8 MPa√mm with a deviation of 1.6% from the analytical solution. The crack propagation rate increases from 2.65×10^{-8} to 3.02×10^{-5} mm/cycle, resulting in a total fatigue life of 8.3 years. These findings emphasize the importance of fracture mechanics-based evaluation to support inspection and maintenance strategies for SPM mooring systems.

Keywords: *Single Point Mooring, mooring chain, fatigue, crack propagation, fracture mechanics, Paris law.*

1. INTRODUCTION

Oil remains the world's primary energy source, with exploration and production activities continuing to expand offshore. Offshore oil distribution infrastructure generally utilizes a Single Point Mooring (SPM) system connected to a Floating Storage and Offloading (FSO) system. The SPM system functions as a floating mooring point, enabling the safe and efficient transfer of oil from subsea pipelines to FSOs or tankers [1].

SPMs are anchored to the seabed using a mooring system consisting of a mooring chain, anchors, and connecting components. The mooring chain is a critical component that withstands dynamic and repeated environmental loads such as waves, currents, and wind, thus inducing cyclic stresses that can lead to material fatigue. Over time, fatigue leads to crack initiation and propagation, potentially compromising structural integrity and leading to mooring system failure [2], [3].

Ardjuna Marine Terminal in the Java Sea is an offshore facility that utilizes an SPM system for oil transfer to FSOs and tankers. The mooring chain at this facility experiences continuous environmental loading, making it susceptible to fatigue failure. Mooring chain failure can disrupt operations, pose safety risks, and potentially cause environmental pollution [4].

A fracture mechanics approach, specifically the Paris Law, can be used to predict crack propagation rates and structural fatigue life based on stress intensity factors [5]. Previous research has shown that the SIF is a key parameter in evaluating crack growth in mooring chains [6], [7]. This study aims to analyze the motion response of the SPM and FSO, determine the maximum stress in the mooring chain, and evaluate crack propagation and fatigue life using fracture mechanics methods.

2. THEORETICAL BASIS

2.1 Theory of Floating Structure Motion

The motion of floating structures is classified into four categories: wave-frequency motion, high-frequency motion, slow-drift motion, and mean drift motion [8]. In the motion response analysis, the concept of Response Amplitude Operator (RAO) is used, which states the ratio of the structure's response amplitude to the incident wave amplitude at each frequency.

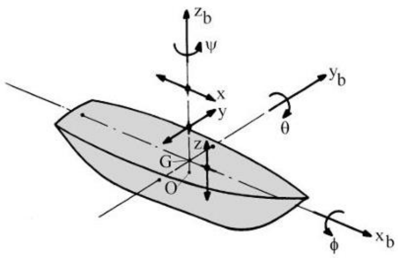

Figure 1. Six Degrees of Freedom

2.2 Tension on the Mooring Chain

According to API RP 2SK [9], the maximum working stress limit on a mooring system is determined by considering the following safety factors.

$$SF = \frac{MBS}{T_{Max}} > 1.67 \quad (1)$$

where MBS is the minimum breaking strength and T max is the maximum tension of the mooring chain. These values determine the safe limit of tensile force before reaching critical conditions.

2.3 Stress intensity factor (SIF)

The stress intensity factor (SIF) is an important parameter in fracture mechanics that is used to assess the stress conditions around the crack tip. For a semi-elliptical crack on the surface, the SIF is expressed by [10]:

$$K_I = 1.12\,\sigma\sqrt{\pi\frac{a}{Q}Mk} \quad (2)$$

where a is the crack depth, σ_Nom is the nominal stress, and Mk and Q are the geometric correction factors.

2.4 Paris Law

The fatigue crack propagation rate is modeled through Paris' Law which states the relationship between the crack growth rate (da/dN) and the stress intensity factor range (ΔK) [11]:

$$\frac{da}{dN} = C(\Delta K)^m \quad (3)$$

where C and m are material constants. Based on British Standard 7910 [12] for steels operating in marine environments with a stress ratio R ≥ 0.5, $C = 5.37\times10^{-14}$ and m = 3.42 are used.

2.4 Location of Cracks in the Mooring Chain

Fatigue cracks in mooring chains generally develop in areas of high stress concentration, namely on the outer surface of the crown, the inner surface of the bend, and the inner side of the straight section of the chain link [13]. These areas are vulnerable because they experience cyclic tensile forces, the effects of contact between the chain links, and geometric influences that cause stress concentrations.

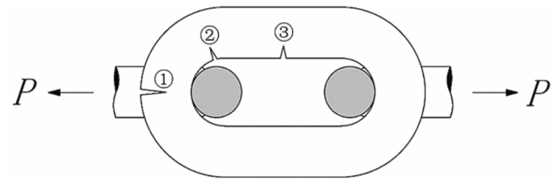

Figure 2. Typical Crack Locations in Mooring Chains

3. METHODOLOGY

3.2 Data Collection

This research was conducted on the SPM and FSO systems at Ardjuna Marine Terminal in the Java Sea. Data collected included general drawings of the SPM and FSO, mooring chain configurations, and environmental data. The environmental parameters used are presented in Table 1.

Table 1. Ardjuna Marine Terminal Environmental Data

Parameter	Value	Unit
Significant Wave Height (Hs)	2.5	m
Wave Period (Tp)	6.3	s
Surface Current Velocity	0.8	m/s
Wind Speed (10 min avg)	12.5	m/s
Water Depth	40	m

3.3 Structural Modeling

The SPM and FSO structural modeling was performed using Modeler software to represent the geometric shapes and hydrostatic characteristics. The main dimensions of both structures are presented in Table 2. After the geometric modeling was completed, hydrostatic adjustment and validation were performed using IACS provisions.

Table 2. FSO General Data

Parameter	SPM	FSO
Length (m)	12.2	234.0
Width (m)	12.2	42.0
Draft (m)	3.5	13.5
Displacement (ton)	580	85,000

3.4 Motion Response Analysis

RAO analysis was performed using Executive software for five wave arrival directions: 0°, 45°, 90°, 135°, and 180°. Motion responses at six degrees of freedom (6DOF) were evaluated to determine the most critical heading conditions. FSO was analyzed under two operating conditions: Full Load and Ballast Load with colinear, non-colinear 1 and non-colinear 2 variations based on DNV-GL-OS-301 [16].

3.5 Mooring Chain Stress Analysis

Stress analysis was performed using Dynamic simulation software, which dynamically models the interaction between environmental loads (waves, currents, wind) and the mooring system. All combinations of environmental load directions were evaluated to obtain the most critical conditions according to API RP 2SK [9] .

3.6 Mooring Chain Crack Analysis

Taking into account the presence of modeled cracks. The analysis was conducted using a finite element-based fracture mechanics approach to determine the structural response and stress field characteristics around the crack tip. The main output of this stage is the stress intensity factor value obtained directly from the finite element analysis software output.

4. ANALYSIS AND DISCUSSION

4.1 Single Point Mooring (SPM) Structural Modeling

Modeling of the Single Point Mooring (SPM) structure was carried out using Modeler software to represent the geometric shape and hydrostatic characteristics of the buoy which functions as the main mooring point of the SPM system.

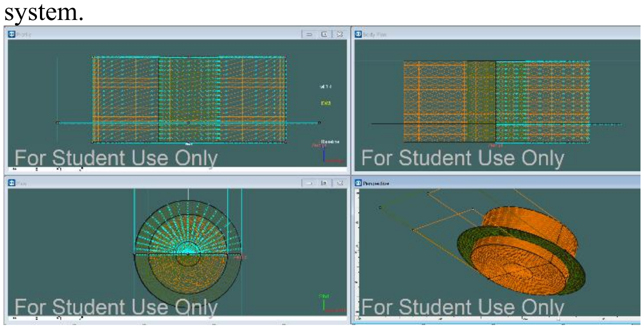

Figure 3. SPM Modelling

According to Figure 4.1, the modeling process begins with the creation of a cylindrical base surface for the buoy, with the addition of a skirt section at the bottom for balancing and increasing displacement. Surface trimming and lofting were then adjusted to ensure a smooth transition between the main body and the skirt section. Once the geometry was finalized, a hydrostatic analysis was performed to verify the displacement values and initial stability of the structure under floating conditions.

4.2 Floating, Storage, and Offloading (FSO) Structural Modeling

Floating Storage and Offloading (FSO) structural modeling was performed using Modeler software to depict the three-dimensional hull shape based on the primary ship geometry data. The primary objective of this modeling is to obtain a realistic and accurate representation of the hull shape, which can be used in subsequent hydrodynamic analyses, particularly in calculating the motion response to ocean waves.

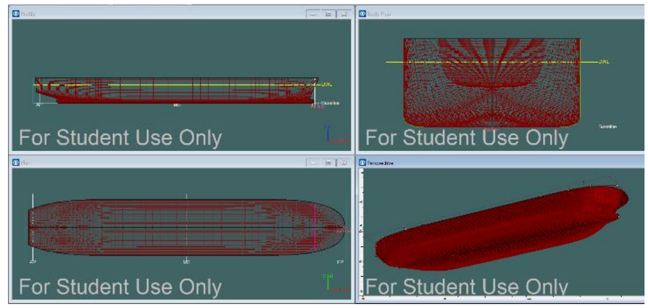

Figure 4. FSO Modelling

Once the geometric model is complete, a hydrostatic adjustment process is performed with displacement volumes to reflect the ship's actual operating conditions. This adjustment is crucial to ensure the model maintains proper balance when analyzing motion responses to marine environmental conditions. With the FSO model geometrically validated, the modeling results will then be used as input in Motion software to analyze the Response Amplitude Operator (RAO).

4.3 Structural Model Validation

Single Point Mooring (SPM) model validation is performed to ensure that the modeling results created using Modeler comply with the geometric and hydrostatic requirements recommended by the International Association of Classification Societies (IACS). This process aims to verify that the SPM model has appropriate dimensions and physical characteristics that represent the actual conditions of the structure in the field.

Table 3. SPM Model Validation

Parameter	Data Value (ton)	Software Value (ton)	Error
Displacement	252.6	250.4	0.871%

Floating Storage and Offloading (FSO) model validation is performed to ensure that the shape and hydrostatic characteristics modeled in Modeler comply with the requirements set by the International Association of Classification Societies (IACS). This validation aims to ensure that the geometry and hydrostatic characteristics of the FSO used in the analysis have a high level of accuracy and are representative of actual conditions in the field.

Table 4. FSO Model Validation

Parameter	Data Value (ton)	Software Value (ton)	Error
Displacement	128938	129393	0.353%
Prismatic Coefficient	0.834	0.84	0.719%
Block Coefficient	0.832	0.833	0.120%
Midship Coefficient	0.997	0.992	0.502%

4.4 Single Point Mooring (SPM) Motion Response Analysis

The RAO analysis was conducted using Executive software, utilizing previously validated SPM and FSO models. Simulations were conducted for five wave directions: 0°, 45°, 90°, 135°, and 180°, to determine the effect of varying wave direction on the structure's motion response across six degrees of freedom (6DOF): surge, sway, heave, roll, pitch, and yaw.

Table 5. Maximum RAO SPM Free Floating Condition

Motion	0°	45°	90°	135°	180°
Surge (m/m)	0.698	0.494	0	0.494	0.698
Sway (m/m)	0	0.495	0.701	0.495	0
Heave (m/m)	1.722	1.669	1.616	1.654	1.695
Roll (°/m)	0	0.371	0.524	0.371	0
Pitch (°/m)	0.521	0.369	0.009	0.369	0.521
Yaw (°/m)	0	0.009	0.013	0.009	0

Overall, these results indicate that the dominant response of the SPM was in the longitudinal direction (surge and pitch) and vertical motion (heave), while the lateral response (sway and roll) was only significant when waves came from the perpendicular direction. The low RAO yaw value confirmed that the SPM mooring system was effective in maintaining directional stability and reducing twisting moments during operating conditions at sea.

4.5 Floating, Storage, and Offloading (FSO) Response Analysis

The Floating, Storage, and Offloading (FSO) RAO analysis was conducted under two operating conditions: Full Load and Ballast Load. This separation is important because changes in load conditions will affect the draft, stability, and mass moment of inertia of the structure, which ultimately impacts the characteristics of the motion response to waves. Simulations were conducted with the same wave incidence directions as the SPM analysis, namely 0°, 45°, 90°, 135°, and 180°, to observe variations in motion response based on the vessel's orientation to the waves.

Table 6. Maximum RAO FSO Full Load Free Floating Condition

Motion	0°	45°	90°	135°	180°
Surge (m/m)	0.876	0.645	0.03	0.645	0.876
Sway (m/m)	0	0.643	0.943	0.643	0
Heave (m/m)	0.92	0.964	1.668	0.964	0.92
Roll (°/m)	0.001	1.829	3.764	1.827	0.001
Pitch (°/m)	0.689	0.775	0.148	0.756	0.682
Yaw (°/m)	0	0.344	0.018	0.357	0

Overall, the RAO results indicate that the 90° wave incidence direction (beam sea) is the most critical condition for the FSO motion response under Full Load conditions, particularly for roll and heave movements. This condition needs to be considered in mooring system design and stability analysis, as it can impact on the operational comfort and safety of the FSO structure when operating on the high seas.

Table 7. Maximum RAO FSO Ballast Load Free Floating Condition

Motion	0°	45°	90°	135°	180°
Surge (m/m)	0.919	0.671	0.01	0.671	0.919
Sway (m/m)	0.001	0.669	0.977	0.669	0.001
Heave (m/m)	0.93	0.964	1.01	0.964	0.93
Roll (°/m)	0.001	1.159	4.903	1.032	0
Pitch (°/m)	0.74	0.747	0.029	0.739	0.737
Yaw (°/m)	0.001	0.327	0.03	0.328	0.001

Based on the maximum RAO table for the FSO under Ballast Load and Free Floating conditions, the FSO's motion response varies depending on the incoming wave direction and the type of motion occurring. In translational motion, the maximum RAO value occurs in surge mode, with a value of 0.919°/m at the 0° and 180° directions, indicating that waves from the fore and aft directions have the greatest influence on longitudinal motion. For sway, the maximum response of 0.977°/m occurs at the 90° direction, indicating that waves from the side most influence lateral motion. Meanwhile, during heave motion, the maximum RAO value of 1.01°/m also occurred at 90°, indicating that side waves exerted the most dominant vertical effect on the structure.

4.6 Mooring Chain Stress Analysis

Mooring chain stress analysis was conducted to determine the maximum tensile force occurring during mooring system operation between the FSO and SPM. The analysis was based on dynamic simulation results using Dynamic simulation software, which models the interaction between environmental loads (waves, currents, and wind) and the mooring system.

Based on API RP 2SK regulations, the maximum working stress limit for a mooring system is determined by considering a safety factor of >1.67 during intake conditions. The mooring safety factor is obtained by comparing the minimum breaking load of the mooring chain with the maximum mooring chain stress.

$$Safety\ Factor = \frac{Minimal\ Breaking\ Load}{Maximum\ Tension} \tag{4}$$

$$Maximum\ Tension = \frac{7051}{1.67} = 4222.16\ \text{kN} \tag{5}$$

This value indicates the maximum safe limit of tensile force that the mooring chain can withstand before reaching a critical breaking point. Therefore, all mooring chain stress analysis results under operating and extreme conditions must be below the limit value of 4222.16 kN for the mooring system to be categorized as structurally safe according to the API RP 2SK design reference.

Table 8. Summary of the four highest stress analysis results on the mooring chain

Mooring Line	Lokasi	Max Tension (kN)	Safety Factor
ML-1	Fairlead	3622.622	1.95
ML-2	Fairlead	3198.450	2.20
ML-3	Fairlead	3045.210	2.32
ML-4	Fairlead	2987.330	2.36
Mean Tension	ML-1	883.06	7.99

4.7 Mooring Chain Modeling and Boundary Conditions

Fatigue modeling in mooring systems states that mooring chain models ideally include at least three links: one main link, half a link for load application, and the other half a link as a retaining component Guidance Note NI 604 DT R00 E [14].

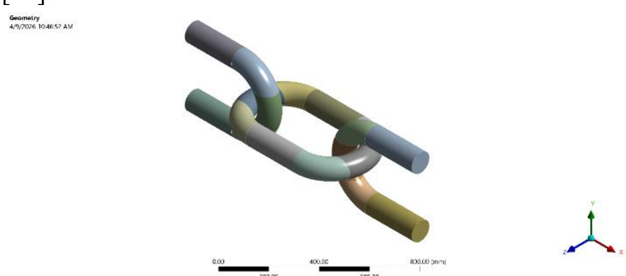

Figure 5. Modelling Mooring Chain

The mooring tensile force is applied to the ends of the chain links through pressure loads acting on specific areas, ensuring an even distribution of the tensile force and representing the actual operating conditions of the mooring chain. On the other hand, the upper surface is set as a fixed boundary condition because in actual conditions, this point is connected to the SPM structure which is much stiffer than the chain. In the local analysis of the mooring chain, the displacement of the SPM structure can be neglected, so the fixed assumption is used to represent the reactions of the global system and avoid rigid body motion in the simulation.

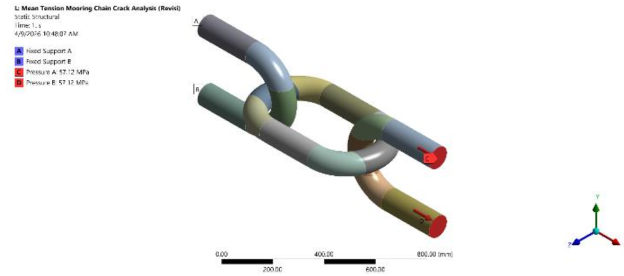

Figure 6. Boundary Condition of Mooring Chain

4.8 Meshing Sensitivity Analysis

In critical mooring chain modeling, a non-uniform meshing strategy was applied, considering the geometric complexity and potential stress concentrations at each link. The crown section was modeled using tetrahedron elements due to its curved geometry and complex cross-sectional changes, requiring element flexibility to accurately represent the shape. Meanwhile, other sections, such as straight segments, were modeled using hexahedron elements, which provide better stress accuracy and numerical stability in relatively simpler geometries.

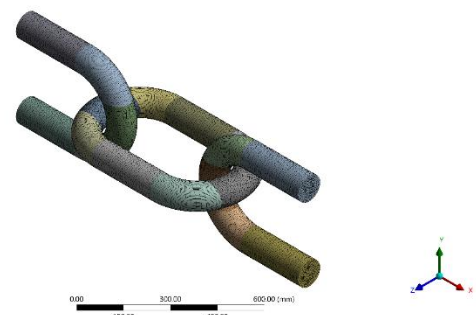

Figure 7. Mooring Chain Meshing Result

The mesh configuration that produced insignificant stress changes with subsequent mesh refinement was selected as the optimal mesh and used in further analysis. The mesh refinement process was stopped when the maximum stress difference between two consecutive mesh levels was less than 2%, indicating convergence.

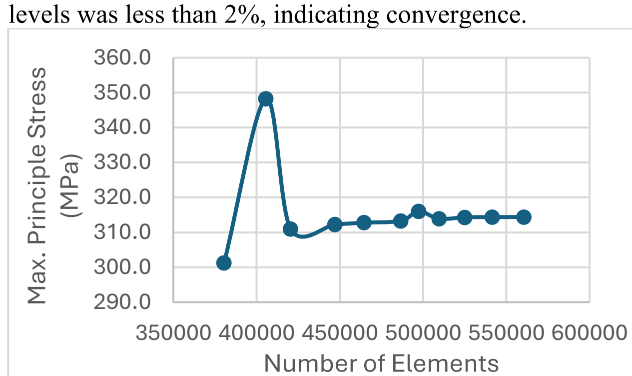

Figure 8. Mooring Chain Meshing Sensitivity

With an element size of 6 mm and a total of 560,616 elements, this value indicates convergence, where the stress difference with respect to the previous mesh refinement is below the 2% tolerance limit of 0.01%.

4.9 Static Structural Analysis Results

Under maximum tension, the maximum principal stress reached 1752.8 MPa, localized on the external surface of the crown. This maximum principal stress exceeded the ultimate strength limit of the material used, indicating that the structure could potentially fail under this maximum tension load. This condition occurred because the maximum stress value obtained from the global dynamic analysis of the mooring line was then applied locally to the three-chain model. Consequently, there was a significant increase in stress concentration on the external surface of the crown, resulting in a stress value much greater than the average loading condition.

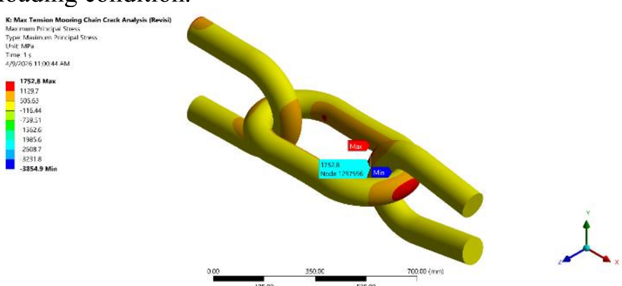

Figure 9. Maximum Principal Stress with Maximum Tension Input

Under mean tension, the maximum principal stress was 427.2 MPa. This value is still below the ultimate strength limit of the material. The stress distribution under this condition also showed the same pattern as under maximum tension, with stress concentration occurring on the external surface of the crown.

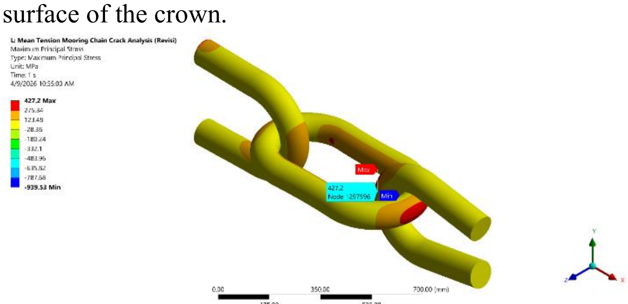

Figure 10. Maximum Principal Stress with Mean Tension Input

In this final project, the static structural analysis was conducted using two loading conditions: maximum tension and mean tension, which were converted to pressure. For subsequent crack analysis, the stress results from the mean tension condition were used as the primary parameter. The selection of mean tension was based on the consideration that this condition represents the operational loading that occurs continuously throughout the mooring chain's service life, making it more relevant for evaluating the potential for crack initiation and propagation due to long-term cyclic loading.

4.10 Semi-Elliptical Crack Modeling

Semi-elliptical crack modeling is a commonly used approach in fracture mechanics analysis to represent surface defects in cylindrical structures, particularly in offshore components subjected to cyclic loading.

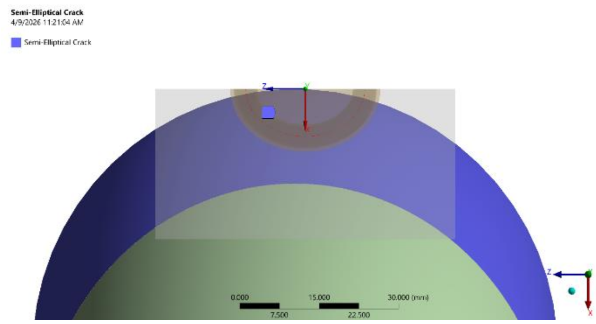

Figure 11. Modelling Semi-elliptical Crack

Figure 11 shows the numerical modeling of a semi-elliptical surface crack in a cylindrical structure, representing a defect caused by fatigue or corrosion. The crack is modeled using a half-ellipse approach, with a local coordinate system (X,Y,Z) to define its orientation and position. The transparent area indicates the analysis domain where the stress concentration and stress intensity factors are evaluated. The dimension scale in millimeters and the color gradient represent the model size and the distribution of field variables. This model is used to analyze crack initiation and propagation under cyclic loading in offshore structures.

4.11 Stress Intensity Factor (SIF) Analysis Results

The SIF (K) calculation was performed in two ways: analytically and using finite element method software. The comparison between both methods shows good agreement, with the percentage error evaluated using the Mean Absolute Percentage Error (MAPE) method being below 10%, indicating that the numerical model provides reliable and accurate results.

Table 9. Comparison of analytical and software Stress Intensity Factor results

Kedalaman Retak a (mm)	Kmax Analitis (MPa√mm)	Kmax FEM (MPa√mm)	Error (%)
0.5	422.648	390.2	7.68%
1.5	732.049	708.77	3.18%
2.5	945.071	925.14	2.11%
3.5	1118.223	1100.7	1.57%
4.5	1267.946	1255.2	1.01%
5.5	1401.767	1395.4	0.45%
6.5	1523.882	1525.6	0.11%
7.5	1636.912	1648.2	0.69%
8.5	1742.626	1764.7	1.27%
9	1793.147	1821.8	1.60%

The significant increase in ΔK with increasing crack depth indicates an acceleration in the nonlinear crack propagation rate, consistent with the fracture mechanics mechanism [6], [15]. These results also indicate that the external surface of the crown is the most critical point because it experiences a combination of axial tensile stress and geometric stress concentration, in accordance with the findings of Bergara et al. [2] and Gemilang et al. [13].

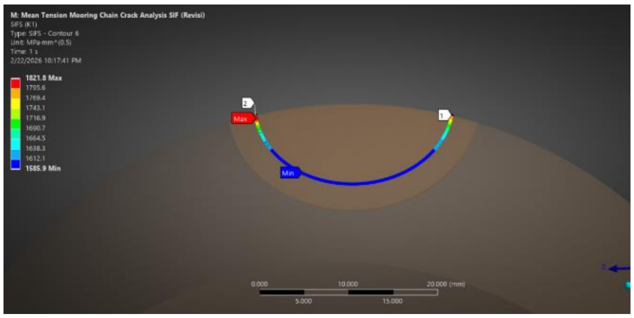

Figure 12. Stress Intensity Factor Results at Maximum Crack Depth of 9 mm

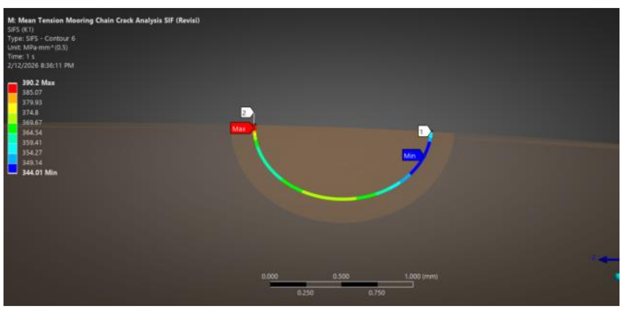

Figure 13. Stress Intensity Factor Results at Initial Crack Depth of 0.5 mm

4.13 Crack Propagation Rate Calculation

The crack propagation rate was calculated using Paris Law with material constants $C = 5.37\times10^{-14}$ and $m = 3.42$ according to British Standard 7910 [12]. The ΔK parameter was obtained from the difference between Kmax and Kmin at each crack depth stage. Table 8 presents the complete results of the crack propagation rate calculation.

Table 10. Crack Propagation Cycle Calculation Results

a (mm)	ΔK (MPa√mm)	da/dN (mm/siklus)	ΔN (siklus)
0,5	46,19	$2{,}65\times10^{-8}$	$3{,}78\times10^{7}$
1,5	59,36	$4{,}81\times10^{-7}$	$2{,}08\times10^{6}$
2,5	84,26	$1{,}38\times10^{-6}$	$7{,}27\times10^{5}$
3,5	105,72	$2{,}72\times10^{-6}$	$3{,}68\times10^{5}$
4,5	127,10	$4{,}72\times10^{-6}$	$2{,}12\times10^{5}$
5,5	149,10	$7{,}62\times10^{-6}$	$1{,}31\times10^{5}$
6,5	171,80	$1{,}17\times10^{-5}$	$8{,}57\times10^{4}$
7,5	195,90	$1{,}73\times10^{-5}$	$5{,}78\times10^{4}$
8,5	221,80	$2{,}51\times10^{-5}$	$3{,}98\times10^{4}$
9,0	235,90	$3{,}02\times10^{-5}$	$3{,}31\times10^{4}$
	Total	$1{,}01\times10^{-4}$	$4{,}15\times10^{7}$

4.14 Fatigue Life Calculation

The fatigue life calculation in this study was conducted using the fracture mechanics method, referring to the empirical relationship of Paris's Law, which states the relationship between the crack propagation rate (da/dN) and the Stress Intensity Factor (ΔK) range. Fatigue life is expressed as the number of loading cycles required for crack growth from its initial size to the final size analyzed.

The accumulated number of cycles across all stages of crack growth yields a total fatigue life of 4.15×10^{7} cycles. This result indicates that most of the structure's fatigue life occurs during the early stages of crack growth, when the crack propagation rate is still relatively low. Therefore, the fatigue life calculation is performed by multiplying the number of cycles by the wave period. The wave period used is 6.3 seconds, and the cycles are converted to annual units as follows.

$$Fatigue\ Life = \frac{N\ \times T}{31563000} \tag{6}$$

$$Fatigue\ Life = \frac{4.15\ \times\ 10^{7} \times 6.3}{31563000} \tag{7}$$

$$Fatigue\ Life = 8.3\ Tahun \tag{8}$$

5. CONCLUSION/SUMMARY

Based on the research results, the following conclusions can be drawn to answer the problem formulation and achieve the objectives of this Final Project.

The highest RAO value for translational motion occurs in the heave response, reaching a maximum of 1.722 at a heading of 0°. For rotational motion, the highest RAO is observed in roll, with a maximum value of 0.524 at a heading of 90°. Under full load conditions, the maximum roll RAO reaches 3.764 °/m at a heading of 90°, whereas under ballast conditions, it increases to 4.903 °/m at the same heading.

Based on the maximum tension analysis of the mooring chain under extreme ballast load in an inline-colinear configuration, the highest tension is recorded in Mooring Line 1 at the fairlead, amounting to 3622.622 kN, with a mean tension of 883.06 kN. All tension values remain below the allowable limit of 4222.16 kN in accordance with API RP 2SK.

For an initial crack depth of 0.5 mm, the stress intensity factor range (ΔK) is 46.19 MPa√mm, resulting in a crack growth rate (da/dN) of 2.647×10^{-8} mm/cycle. As the crack depth increases to 9 mm, ΔK rises to 235.9 MPa√mm, and the crack growth rate significantly accelerates to 3.019×10^{-5} mm/cycle. The total fatigue life of the mooring chain is estimated to be 8.3 years.

ACKNOWLEDGEMENTS

The author would like to thank the Department of Ocean Engineering, Faculty of Ocean Technology, Sepuluh Nopember Institute of Technology for the academic support and research facilities provided, as well as to all parties who have contributed to the completion of this research.

REFERENCES

[1] Y. Wang, H. Xie, dan E. Zheng, "Design and research on optimization of single point mooring system," J. Phys. Conf. Ser., vol. 1303, no. 1, 2019. https://doi.org/10.1088/1742-6596/1303/1/012031

[2] A. Bergara, A. Arredondo, J. Altuzarra, dan J. M. Martínez-Esnaola, "Fatigue crack propagation analysis in offshore mooring chains and the influence of manufacturing residual stresses," Ocean Eng., vol. 257, 2022. https://doi.org/10.1016/j.oceaneng.2022.111605

[3] V. Hellum, Ø. Gabrielsen, dan S. Kyrre, "Fatigue crack growth in mooring chain steel at different mean load levels," Mar. Struct., vol. 92, 2023. https://doi.org/10.1016/j.marstruc.2023.103507

[4] Y. Bai dan Q. Bai, Subsea Engineering Handbook, vol. 17. 2012.

[5] X. Gao, X. Liu, X. Xue, dan N. Z. Chen, "Fracture mechanics-based mooring system fatigue analysis for a spar-based floating offshore wind turbine," Ocean Eng., vol. 223, 2021. https://doi.org/10.1016/j.oceaneng.2021.108618

[6] M. Aursand dan B. H. Skallerud, "Mode I stress intensity factors for semi-elliptical fatigue cracks in curved round bars," Theor. Appl. Fract. Mech., vol. 112, 2021. https://doi.org/10.1016/j.tafmec.2021.102904

[7] X. Xue, N. Chen, Y. Pu, dan X. Gao, "Fracture mechanics analysis for mooring chain links subjected to out-of-plane bending," Mar. Struct., vol. 71, 2020. https://doi.org/10.1016/j.marstruc.2020.102740

[8] O. M. Faltinsen, Sea Loads on Ships and Offshore Structures. Cambridge: Cambridge University Press, 1990.

[9] API RP 2SK, Design and Analysis of Stationkeeping Systems for Floating Structures. American Petroleum Institute, 2015.

[10] D. Broek, Elementary Engineering Fracture Mechanics. 1986.

[11] J. Barsom dan S. Rolfe, Fracture and Fatigue Control in Structures: Applications of Fracture Mechanics, 3rd ed. ASTM International, 2008.

[12] British Standard 7910, Guide to Methods for Assessing the Acceptability of Flaws in Metallic Structures. British Standards Institute, 2019.

[13] G. M. Gemilang, P. A. S. Reed, dan A. J. Sobey, "Selection of appropriate numerical models for modelling the stresses in mooring chains," Mar. Struct., vol. 75, 2021. https://doi.org/10.1016/j.marstruc.2020.102864

[14] Bureau Veritas, Guidance Note NI 604 DT R00 E: Fatigue of Top Chain of Mooring Lines due to In-plane and Out-of-plane Bendings. 2014.

[15] K. Yuan, L. Li, dan K. Dong, "General point load weight function for semi-elliptical surface cracks in round bars," Theor. Appl. Fract. Mech., vol. 129, 2024. https://doi.org/10.1016/j.tafmec.2023.104209

[16] DNVGL-OS-E301, Offshore Standards - Position Mooring. Det Norske Veritas - Germanischer Lloyd, 2018.